HHS Public Access

Author manuscript

Cancer Immunol Res. Author manuscript; available in PMC 2020 October 01.

Published in final edited form as:

Cancer Immunol Res. 2020 April ; 8(4): 465–478. doi:10.1158/2326-6066.CIR-19-0449.

CD73 blockade promotes dendritic cell infiltration of irradiated tumors and tumor rejection

Erik Wennerberg[1], **Sheila Spada**[1], **Nils-Petter Rudqvist**[1], **Claire Lhuillier**[1], **Sylvia Gruber**[1,4], **Qiuying Chen**[2], **Fengli Zhang**[2], **Xi Kathy Zhou**[3], **Steven S. Gross**[2], **Silvia Chiara Formenti**[1], **Sandra Demaria**[1]

[1]Department of Radiation Oncology, Weill Cornell Medicine, New York, NY, USA.

[2]Department of Pharmacology, Weill Cornell Medicine, New York, NY, USA.

[3]Division of Biostatistics and Epidemiology, Department of Healthcare Policy and Research, Weill Cornell Medicine, New York, NY, USA

[4]Department of Radiation Oncology, Medical University of Vienna, Vienna, Austria

Abstract

The ability of focal radiotherapy to promote priming of tumor-specific $CD8^+$ T cells and increase responses to immunotherapy is dependent on infiltration of the tumor by Batf3-dependent conventional dendritic cell type 1 (cDC1) cells. Such infiltration is driven by radiotherapy-induced IFN type I (IFN-I). Other signals may also modulate cDC1 infiltration of irradiated tumors. Here we found increased expression of adenosine-generating enzymes CD38 and CD73 in irradiated mouse and human breast cancer cells and increased adenosine in mouse tumors following radiotherapy. CD73 blockade alone had no effect. CD73 blockade with radiotherapy restored radiotherapy-induced cDC1 infiltration of tumors in settings where radiotherapy induction of IFN-I was suboptimal. In the absence of radiotherapy-induced IFN-I, blockade of CD73 was required for rejection of the irradiated tumor and for systemic tumor control (abscopal effect) in the context of CTLA-4-blockade. These results suggest that CD73 may be a radiation-induced checkpoint, and that CD73 blockade in combination with radiotherapy and immune checkpoint blockade might improve patient response to therapy.

Corresponding author: Sandra Demaria, Department of Radiation Oncology, Weill Cornell, Medicine, New York, NY 10065, USA. szd3005@med.cornell.edu; Phone: 646-962-2092.

Author contributions:

E.W. designed the experiments and contributed to overall study design, and performed the experiments and data analysis. S.D. conceived the study and wrote the manuscript together with E.W. F.Z, C.Q. and S.S.G aided in design, performed and aided in data analysis of LC-MS/MS experiments. X.K.Z. supervised statistical analysis. N-PR, C.L., S.S. and S.G. contributed to perform experimental work and aided in data analysis. S.C.F. edited the manuscript. All authors approved the final version of the manuscript.

Potential conflicts of interest:

The authors declare no competing financial interests directly related to this manuscript. SCF's daughter is an attorney (paid consultant) at Pfizer. SCF reports receiving a commercial research grant from Bristol Myers Squibb, Varian, Merck, Regeneron, and Eisai, and has received speakers bureau honoraria from Varian, Eisai, AstraZeneca, Merck, Viewray, Bayer, and EMD Serono. S.D is a scientific advisory board member (paid consultant) at Lytix Biopharma, is an Ad hoc consultant at AstraZeneca, Mersana Therapeutics, and EMD Serono, and reports receiving a commercial research grant from Lytix Biopharma and Nanobiotix.

Keywords

Adenosine; CD73; Breast cancer; Dendritic cells; Radiation therapy

Introduction

In patients with pre-existing antitumor immunity, immune checkpoint blockade (ICB) therapy with antibodies targeting cytotoxic T-lymphocyte-associated protein 4 (CTLA-4) and programmed cell death 1 (PD-1) or its ligand PDL-1 has shown clinical efficacy. Such therapy unleashes the effector function of tumor-specific $CD8^+$ T cells (1). However, ICB therapy is ineffective for most patients, prompting the search for strategies that work in concert with ICB to immunize the patients against their tumor (2). Focal radiotherapy can elicit antitumor T cell responses in combination with ICB in multiple ICB-resistant mouse tumor models (reviewed in (3)). The combination of radiotherapy and ICB is also being tested in the clinic (4). Success is variable (5,6), emphasizing the need to optimize the use of radiotherapy to generate antitumor T cell responses and enhance responses to ICB therapy (7).

Mechanistic studies have revealed a role of the IFN type I (IFN-I) pathway in radiotherapy immunogenicity (8–10). In poorly immunogenic tumors, cancer cell-intrinsic IFN-I production promotes tumor infiltration by conventional dendritic cells type 1 (cDC1), a subset of DCs whose ontogeny is dependent on the transcription factor basic leucine zipper transcription factor ATF-like (Batf3) (9). cDC1, which cross-present tumor antigens to $CD8^+$ T cells, are essential for antitumor immune responses (11). Radiotherapy-induced T cell priming was abrogated in Batf3-deficient ($Batf3^{-/-}$) mice (9). IFN-I was implicated in the synergistic and abscopal response of patients with metastatic lung cancer who were treated with both ipilimumab and radiotherapy (6). Induction of IFN-I by radiotherapy is mediated via the cyclic GMP-AMP synthase (cGAS) through the stimulation of interferon genes (STING) pathway, which is frequently downregulated in tumors (9,10,12). Here, we search for alternative pathways to promote radiotherapy-induced cDC1 infiltration.

The pro-inflammatory molecule ATP is released from cells undergoing radiation-induced cell death (13), and promotes the recruitment and activation of DC (14, 15). Extracellular ATP concentrations are tightly regulated by ectoenzymes, which are often overexpressed in tumors (16). Following hydrolysis of ATP into ADP and AMP by the ectonucleotidase CD39, AMP is irreversibly de-phosphorylated into adenosine by CD73. Adenosine can also be generated by conversion of NAD^+ into ADP-ribose (ADPR) and AMP by CD38 and CD203a (17,18). .

Adenosine elicits multiple anti-inflammatory and immunosuppressive effects, mediated by the adenosine receptors A1, A2A, A2B and A3 expressed on immune cells (19). These effects include promoting a tolerogenic phenotype in DCs with reduced ability to induce Th1 polarization of naïve T cells (20), inducing T cell anergy and promoting regulatory T cell (Treg) differentiation (21). Elevated expression of CD73 is associated with a poor prognosis in triple-negative breast cancer (TNBC) and other tumor types (22–24). Elevated tumor expression of CD38 has been observed in melanoma (17) and is implicated in

acquired resistance to anti-PD-1 therapy (25). The therapeutic potential of blocking adenosine pathways with monoclonal antibodies (mAB) targeting CD73 and small molecule inhibitors of A2AR is being tested in phase I trials in patients with solid tumors (16,26).

Here we investigated how adenosine regulates radiation-induced immune responses. We found that expression of CD73 and ectonucleotidases was upregulated by radiation in human and mouse breast cancer cells. Adenosine content was increased in irradiated tumors. CD73 blockade enhanced (i) tumor infiltration by cDC1 in the absence of radiation-induced IFN-I, (ii) response of the irradiated tumor, and (iii) induction of systemic antitumor T cell responses.

Materials and Methods

Tumor cells and reagents

BALB/c-derived mammary carcinoma cell lines TSA and 4T1 were obtained from Dr. Lollini and Dr. Miller respectively (27,28) in 2002, and authenticated by IDEXX Bioresearch (Columbia, MO, USA) in 2019. Human TNBC cells MDA-MB-231 and 4175TR were purchased from ATCC and obtained from Dr. Massague, respectively, and were authenticated in 2016 by IDEXX Bioresearch. Cells were screened for *mycoplasma* using the Lookout mycoplasma detection kit (Sigma) prior to preparation of working stocks of frozen cells, and thawn 3 to 5 days before use in all experiments… Tumor cells were grown in DMEM (Gibco) cell culture medium supplemented with 10% FBS, 2mol/L L-glutamine, 100U/ml penicillin, 100μg/ml streptomycin, and 2.5×10^{-5} mol/L β-mercaptoethanol (Life Technologies) (complete medium). Rat mAb to mouse CD73 (TY/23, BE0209), rat IgG2a isotype control (2A3, BE0089), and hamster mAb to -mouse CTLA-4 (9H10, BE0131) were purchased from BioXcell.

Animals

Wild-type (WT) BALB/c female mice were purchased from Taconic farms (Germantown, NY, USA). BALB/c interferon-α/β-receptor-1-deficient ($Ifnar1^{-/-}$) mice were provided from Dr. Durbin, Rutgers University. BALB/c $Batf3^{-/-}$ mice were purchased from Jackson laboratories and bred in house. All mice were maintained under pathogen-free conditions in the animal facility at Weill Cornell Medicine or New York University School of Medicine. All mouse experiments were approved by the Institutional Animal Care and Use Committee (IACUC) of each institution.

Generation of tumor cells with cGAS and CD73 knockdown

TSA cells expressing a tetracycline-inducible shRNA targeting cGAS (TSA^{shcGAS}) or a non-silencing construct (TSA^{shNS}) have been previously described (9). TSA^{shCD73} were prepared using a similar protocol. Briefly, HEK293-FT cells were transfected with the packaging plasmids pPAX2 and pMD2 and a pTRIPZ vector containing a tetracycline-inducible promoter driving the expression of a TurboRFP fluorescent reporter (GE Dharmacon technology). Short-hairpin RNA (shRNA) directed against CD73 mRNA (*Nt5e*, mouse-shRNA: AAGCATGACTCTGGTGATCAAG) was cloned into pTRIPZ using EcoRI

and XhoI restriction sites. TSA cells were transduced with cell-free virus-containing supernatants and selected with 4μg/ml of puromycin during 48 hours.

Mouse tumor challenge and treatment

BALB/c mice were inoculated with 1×10^5 TSA, TSA^{shCD73}, TSA^{shcGAS}, TSA^{shNS} or with 5×10^4 4T1 cells respectively by subcutaneous (s.c.) injection in the right flank (primary tumor). In some experiments, BALB/c mice were injected s.c. in the contralateral flank with TSA or TSA^{shNS} cells (abscopal tumor) two days following primary tumor inoculation. When applicable, cGAS or CD73 knockdown was induced by administration of doxycycline (100μg/ml) in drinking water *ad libitum* starting 4 days prior to treatment start, which was replenished every 4 days until day 28 and 30, respectively. Mice were randomized to treatment groups when primary tumors reached an average tumor volume of 40–60mm^3 and abscopal tumors reached an average tumor volume of 15–20mm^3. All mice (including mock-irradiated mice) were anesthetized by intraperitoneal (i.p.) injection of Avertin (240mg/kg). Using the Small Animal Radiation Research Platform (SARRP, Xstrahl, Surrey, UK), radiotherapy was delivered at 271cGy/min directed to the primary tumor as a single dose of 8, 12 or 20 Gy or with 3 fractions of 8 Gy delivered on consecutive days (8 Gy×3). Anti-CD73 was administered i.p. in 4 doses of 100μg 3 days apart starting the day prior to radiotherapy. Anti-CTLA-4 was administered i.p. in 3 doses of 200μg 3 days apart starting on the last day of radiotherapy. Tumors were measured by caliper every 2–3 days and volumes calculated using the formula: length × $width^2$ × π/6. Mice were sacrificed when tumor exceeded 1000 mm^3 or if animals showed signs of distress.

Assessment of lung metastatic burden in 4T1 tumor model

BALB/c mice were sacrificed at day 19 after start of treatment. Mouse lungs were excised and fixed in 4% paraformaldehyde for 24 hours. Lung sample treatments were blinded to investigators and gross lung metastases were enumerated using a dissection microscope.

Preparation of cells for flow cytometry analysis

Human and murine tumor cells were cultured until 80% confluent. Cells were either mock-irradiated (0 Gy) or treated with 8, 12, 20 Gy or 8 Gy×3. The culture medium was replaced with fresh medium after radiotherapy and incubated for 24 hours after which cells were trypsinized and single cell suspensions were washed in PBS before staining. Mouse flank tumors were excised, weighed and single cell suspensions were generated following digestion using a tumor dissociation kit (Miltenyi, 130-096-730) and the GentleMACS Octo dissociator (Miltenyi). Single cell suspensions from tumors were strained through a 70μM filter before staining.

Flow cytometry analysis

Cells were stained with fixable viability dye in PBS, 20 min, 4°C, then stained for surface markers using fluorochrome-conjugated antibodies (listed in Supplementary Table S1) for 20 min, 4°C. Cells were fixed using the cytofix/Cytoperm kit (BD Biosciences, 554714) followed by staining for intracellular targets. Samples were acquired on LSRII (BD Biosciences) or MACSQuant (Miltenyi) flow cytometers and analyzed using FlowJo

software (Tree Star). Tregs were identified as $CD4^+CD25^+FoxP3^+$, DCs were identified as $CD11c^+MHCII^+$ or $CD11c^+$, and cDC1 in the DC population were identified by expression of CD103, XCR1, and/or CD8α. To account for changes in autofluorescence induced by treatment, for each sample the mean fluorescence intensity (MFI) of antibody-stained cells was corrected for the MFI of cells stained with fluorescence minus one (FMO) as indicated.

Immunostaining of tumor tissue and image acquisition

Subcutaneous mouse tumors were fixed in 4% paraformaldehyde for 24h at 4°C , placed in 30% sucrose solution for 24h, and frozen in optimal cutting temperature (O.C.T.) compound (Sakura Finetek). Tissue sections (7 μM) were incubated with PBS containing 50mM glycine for 15 min, followed by permeabilization with PBS containing 0.05% Tween (Sigma) and 0.01% Triton-X (FisherBiotech). Tumor sections were blocked with PBS containing 1% BSA and 5% goat serum for 1 hour and stained with primary antibodies (listed in Supplementary Table S1) at 4°C overnight. Tumor sections were stained with secondary antibodies (listed in Supplementary Table S1) for 1 hour and mounted with DAPI-containing mounting medium (Vector Laboratories). Images of tumor sections were acquired using the Axio Observer Inverted Fluorescence microscope (Zeiss).

Adoptive transfer experiments

Bone marrow cells isolated from tibia and femur of WT or $Ifnar^{-/-}$ BALB/c mice were plated in petri dishes (Fischer Scientific) in RPMI 1640 (Gibco) complete medium containing 3% granulocyte-macrophage colony-stimulating factor (GM-CSF) (generated from GM-CSF cell line (29)) and 200ng/ml FMS-like tyrosine kinase 3 ligand (FLT3L) (eBioscience) and 20ng/ml IL-4 (eBioscience) to generate cDC1 (30). On day 14–16 of culture, cells were analyzed by flow cytometry for cDC1 percentage, which was consistently >80%, and labeled with carboxyfluorescein (CFSE) (CellTrace™ CFSE Cell Proliferation Kit, Invitrogen, C34554). $Batf3^{-/-}$ mice or WT mice bearing primary and abscopal TSA tumors (60–70mm^3) received focal radiotherapy to the primary tumor either as a single dose of 20 Gy or 8 Gy× 3. Two hours prior to the last radiotherapy dose, mice were injected i.p. with anti-CD73 or isotype control mAb. Six hours following the last radiotherapy dose, all mice received intravenous (i.v.) injections of CFSE-labeled cDC1s (1×10^6 cells/mouse). After 48 hours, irradiated and non-irradiated tumors were harvested, homogenized into single cell suspensions as described above and analyzed by flow cytometry for infiltration of CFSE-labeled cDC1. Gating strategy is described in Supplementary Fig. S1.

Extraction of tumor metabolites for analysis by liquid chromatography-mass spectrometry (LC/MS)

Mouse tumors were excised and immediately snap-frozen. Tumor tissues were washed twice with ice-cold PBS, followed by metabolite extraction using −70°C 80% methanol in water (LC/MS grade methanol, Fisher Scientific, Grand Island, NY). The tissue–methanol mixture was subjected to bead-beating for 45s using a Tissuelyser cell disrupter (Qiagen). Extracts were centrifuged for 5 min at 5,000r.p.m. to pellet insoluble material and supernatants were transferred to clean tubes. The extraction procedure was repeated two additional times and all three supernatants were pooled, dried in a Vacufuge (Eppendorf) and stored at −80°C until analysis. The methanol-insoluble protein pellet was solubilized in 0.2M NaOH at 95°C

for 20 min and quantified using the Bio-Rad DC assay (Bio-Rad). On the day of metabolite analysis, dried cell extracts were reconstituted in 70% acetonitrile with 0.2% ammonium hydroxide at a relative protein concentration of 4μg/ml and 4μl of the reconstituted extract was injected for LC/MS-based untargeted metabolite profiling.

LC/MS analysis of adenosine in tumors

Metabolomic analysis was performed on tumor extracts by LC/MS as described previously (31), using a platform comprised of an Agilent Model 1290 Infinity II liquid chromatography system coupled to an Agilent 6550 iFunnel time-of-flight MS analyzer. Chromatography of polar metabolites was performed using aqueous normal phase (ANP) chromatography on a Diamond Hydride column (Microsolv, Eatontown, NJ). Mobile phases consisted of: (A) 50% isopropanol, containing 0.025% acetic acid, and (B) 90% acetonitrile containing 5 mM ammonium acetate. To eliminate the interference of metal ions on chromatographic peak integrity and electrospray ionization, EDTA was added to the mobile phase at a final concentration of 6μM. The following gradient was applied: 0–1.0 min, 99% B; 1.0–15.0 min, to 20% B; 15.0 to 29.0, 0% B; 29.1 to 37 min, 99% B. Raw LC/MS data were extracted by MassHunter Profinder 8.0 and compared with a pure adenosine standard using MassProfiler Professional 14.9 software and a default data normalization method of median baselining and LOG2 transformation (Agilent technologies, Santa Clara, CA).

Soluble CD73 (sCD73) measurement by ELISA

Plasma samples from metastatic breast cancer patients participating in a prospective randomized trial assessing the efficacy of the anti-TGFβ fresolimumab in combination with radiotherapy (7.5Gy×3) (NCT01401062, ref (32)) were analyzed for concentration of sCD73 by ELISA (Abcam, ab213761). . Concentration of sCD73 was measured in samples collected before treatment (baseline) and at week two, after completion of radiotherapy administered during week one. Supernatants from MDA-MB-231 and 41745TR tumor cells mock-treated or irradiated with 8 Gy×3 were harvested 24h after treatment, and measured for sCD73 by ELISA. sCD73 concentrations were normalized to the viable cell count at the time of supernatant harvest.

Statistical Analysis

Differences in mouse tumor volume (log transformed) between treatment groups was evaluated using repeated measures ANOVA from start of treatment until the indicated timepoints. Mouse survival was illustrated using the Kaplan-Meier method and differences in survival between treatment groups were evaluated using the Log Rank-test. Differences in frequency of intratumoral cell populations and MFI values between treatment groups were calculated using ANOVA and Tukey's test was applied for pairwise comparisons between treatment groups. Differences in adenosine abundance and tumor infiltration of adoptively transferred cDC1 between treatment groups was calculated using Welch's t-test. When appropriate, data were log2 or square root transformed prior to statistical analysis to ensure the underlying model assumptions were satisfied. Percentage of change in sCD73 plasma concentration was analyzed using a one-sample *t* test. Statistical analysis was performed using Prism version 8 (Graphpad). All statistical tests performed were two-tailed and p-

values of <0.05 were considered as statistically significant. Except where indicated, all data shows mean ± standard error of the mean (s.e.m.).

Results

Radiation increases ectonucleotidases that generate adenosine in mouse breast tumors

Adenosine is induced in response to tissue damage and inflammation (33), thus we hypothesized that radiation-induced damage to the tumor could lead to an increase in adenosine concentration. To test the effects of radiation on adenosine concentration within the tumor microenvironment, BALB/c mice bearing syngeneic s.c. TSA mammary carcinoma were treated with focal radiotherapy and tumors were analyzed 24 hours later. Irradiation, did not have a significant effect on adenosine concentrations until treatment with 20 Gy (148 % mean increase over untreated control tumors; Fig. 1A).

To explore the mechanisms of this adenosine increase, we analyzed tumor expression of the ectonucleotidases CD39 and CD73 in the $CD45^-$ and $CD45^+$ compartment, the latter representing from 23 to 36% of total viable cells, with no statistically significant differences between the groups. At 24 hours after radiotherapy, CD39, which was expressed only by $CD45^+$ cells, did not show significant changes (Fig. 1B–C). CD73 was expressed by a subset of $CD45^+$ cells and its expression did not change in irradiated tumors. In contrast, most $CD45^-$ cells expressed abundant CD73 in untreated tumors and increased expression after treatment with 20 Gy radiotherapy (Fig. 1D–E).

Given the effect of radiotherapy on the expression of CD73 in the $CD45^-$ compartment of TSA tumors *in vivo*, we sought to investigate the effects of radiation on the expression of the ectonucleotidases that generate adenosine *in vitro*. Expression of CD39 was not detectable on TSA or on 4T1 mouse mammary carcinoma cells (Supplementary Fig. S2A), whereas CD73 was expressed and upregulated by radiation. TSA and 4T1 cells also expressed CD38 and CD203a, the two members of the non-canonical adenosine pathway and CD38 was significantly upregulated by radiation in both cell lines (Fig. 2A–D). In 4T1 cells CD203a expression was significantly upregulated after radiation (Fig. 2C–D). These data show that radiation induces this immunosuppressive pathway.

Radiation increases CD73 expression and release in human breast cancer

To investigate if human breast cancer cells respond to radiation by upregulating the ectonucleotidases that generate adenosine, we treated the human TNBC cell lines MDA-MB-231 and 4175TR with various radiation doses and analyzed them for expression of CD38 and CD73. Similar to mouse breast cancer cells, both MDA-MB-231 and 4175TR cells were negative for CD39 (Supplementary Fig. S2B) and showed a significant increase in surface expression of CD38 and CD73 at all radiation doses tested. The largest increase in expression of CD38 was seen after 8 Gy×3 radiotherapy (Fig. 3A and Supplementary Fig. S3).

CD73 is shed following substrate binding and is detectable in the circulation. Soluble CD73 (sCD73) amounts are associated with poor prognosis in melanoma patients, suggesting that circulating sCD73 reflects an immunosuppressive tumor microenvironment (34,35). To test

whether the increased cell surface expression of CD73 induced by radiation on human breast cancer cells is associated with an increase in shedding, sCD73 concentrations were measured in the supernatants of MDA-MB-231 and 4175TR cells treated with 8 Gy×3, a radiation regimen similar to that used in breast cancer patients (32). sCD73 amounts were significantly increased after treatment of MDA-MB-231 with 8 Gy×3 (Fig. 3B) with similar effects on 4175TR cells (Supplementary Fig. S3B).

Next, we explored the effects of radiotherapy on upregulation of the ectonucleotidases that generate adenosine in breast cancer patients. Given that increased amounts of surface CD73 were associated with increased sCD73 in *in vitro* irradiated breast cancer cells, we measured sCD73 amounts in plasma samples available from 15 metastatic breast cancer patients who were treated in a clinical study testing the combination of radiotherapy (7.5Gy×3) with the TGFβ-neutralizing antibody fresolimumab (32). Six patients had TNBC, 7 patients had hormone receptor-positive (HR^+) $HER2^-$ breast cancer, 1 had HR^+HER2^+ breast cancer and one had HR^-HER2^+ breast cancer. No objective responses were observed in this trial, although patients randomized to the higher dose of fresolimumab experienced better survival (32). Concentrations of sCD73 were significantly increased from baseline at week 2, shortly after completion of radiotherapy (Fig. 3C). This increase was similar in patients receiving 1mg/kg or 10 mg/kg fresolimumab ($P = 0.732$). Although an effect of fresolimumab on sCD73 concentrations cannot be excluded, TGFβ enhances expression of CD73 (36), thus it is unlikely that TGFβ-blockade is responsible for increased sCD73. Five of 6 patients with TNBC, but only 3 of 7 patients with HR^+HER2^- breast cancer showed increased sCD73 at week 2 compared to baseline, but the numbers are too small to suggest a differential response dependent on tumor subtype.

Blocking adenosine generation enhances tumor response to 20 Gy radiotherapy

To test the consequences of radiation-induced adenosine generation in the tumor microenvironment, anti-CD73 was administered to mice in conjunction with focal radiotherapy (Fig. 4A). A single dose of 20 Gy radiotherapy was administered because this dose induced the most consistent increase in tumor concentration of adenosine *in vivo* in the TSA model (Fig. 1A), and the highest amounts of CD73 on TSA cells (Fig. 2B). Despite baseline expression of CD73 on TSA cells, CD73 blockade had no significant effect on tumor progression and survival in non-irradiated mice. In combination with radiotherapy, CD73 blockade enhanced tumor response and extended mice survival, with 2/7 mice showing complete tumor regression (Fig. 4B–C). To determine whether the activity of the combination treatment was due to CD73 blockade on the cancer cells and/or the tumor stroma, TSA cells were transduced with a doxycycline-inducible shRNA construct targeting CD73 (TSA^{shCD73}). After knockdown was confirmed (Supplementary Fig. S4A), TSA^{shCD73} and TSA cells expressing a non-silencing construct (TSA^{shNS}) were implanted into mice. Six days later mice were given doxycycline to induce CD73 knockdown followed by treatment with 20 Gy radiotherapy (Supplementary Fig. S4B). Without radiation, CD73 knockdown did not affect tumor growth. With radiation (20 Gy), CD73 knockdown improved tumor response to the same extent as antibody-mediated blockade of CD73 in mice bearing TSA^{shNS} tumors (Supplementary Fig. S4C). Addition of anti-CD73 to mice bearing TSA^{shCD73} and treated with radiotherapy did not further improve tumor control or

mice survival (Supplementary Fig. S4D), indicating that CD73 expressed by the cancer cells is the target limiting the response to radiotherapy.

To dissect the mechanisms responsible for tumor control by the combination of radiotherapy and CD73 blockade, the immune infiltrate was analyzed a week after beginning of treatment. CD73 blockade alone had no effect, but when used with 20 Gy radiotherapy, it increased the cDC1 subset (identified by CD8α expression) of intratumoral DCs and their expression of the maturation marker CD86 (Fig. 4D–E). These results were confirmed using the cDC1 marker CD103 and CD40 as a maturation marker (Supplementary Fig. S5). Analysis of the T cell compartment revealed an increase in $CD8^+$ T cells in tumors of mice treated with 20 Gy and CD73 blockade (Fig. 4F). Expression of CD69, a marker of T cell activation and tissue-resident differentiation, was enhanced in $CD8^+$ T cells within irradiated tumors, and further enhanced by CD73 blockade (Fig. 4G). Treg cells were significantly increased by 20 Gy radiotherapy, consistent with the previously observed increase in Treg after tumor irradiation with a similar single radiotherapy dose (37), but this increase was abrogated by CD73 blockade (Fig. 4H). The ratio of $CD8^+$ to Treg cells, a parameter associated with effective tumor rejection in response to immunotherapy (38), was significantly increased only in tumors of mice treated with radiotherapy and CD73 blockade (Fig. 4I).

Next, we investigated the kinetics of DC infiltration in irradiated tumors in response to CD73 blockade (Supplementary Fig. S6). A significant change in cDC1 numbers over time was seen only in tumors of mice treated with both 20 Gy radiation and CD73 blockade: change was evident at day 4 and increased at day 6 (Supplementary Fig. S6B). Immunostaining of tumor sections confirmed the presence of cDC1 cells inside the tumor and showed that some DCs formed clusters with T cells (Supplementary Fig. S6 C–D).

Overall, these results indicate that targeting CD73 in mice bearing TSA tumors has no effect by itself but acts in synergy with radiotherapy to improve tumor infiltration by cDC1 and T cells and to promote tumor rejection.

cDC1 induce antitumor immune responses to treatment with CD73 blockade and 20 Gy radiotherapy

Radiotherapy-induced infiltration of TSA tumors by cDC1 primes antitumor $CD8^+$ T cell responses to 8 Gy×3 radiotherapy, but does not occur when tumors are treated with a single dose of 20 Gy radiotherapy due to poor induction of IFN-I by this radiotherapy dose (9). Given the enrichment of cDC1 and $CD8^+$ T cells in TSA tumors treated with the combination of 20 Gy radiotherapy and CD73 blockade (Fig. 4D, F and Supplementary Fig. S5), we asked whether the synergy of 20 Gy and CD73 blockade was cDC1-dependent. We used $Batf3^{-/-}$ mice that lack cDC1 as recipient of TSA cells. . The synergy between 20 Gy radiotherapy and CD73 blockade was abrogated in $Batf3^{-/-}$ mice (Fig. 5A). Consistent with the inability of these mice to activate antitumor $CD8^+$ T cells, the intratumoral $CD8^+$:Treg cell ratio was not increased in $Batf3^{-/-}$ mice treated with 20 Gy and CD73 blockade (Fig. 5B). Expression of CD69 by $CD8^+$ T cells was induced by radiotherapy but not further increased by CD73 blockade (Fig. 5C), indicating that the effects of CD73 blockade are dependent on cDC1.

To test the ability of 20 Gy radiotherapy to elicit signals that promote tumor infiltration by cDC1 when CD73 is blocked, we generated cDC1 *ex vivo* by culture of bone marrow cells from WT BALB/c mice with FLT3L and GM-CSF as previously described (30). Obtained cDC1s were labeled with CFSE and injected i.v. into Batf3$^{-/-}$ mice bearing two TSA tumors in opposite flanks 6 hours after irradiation of one tumor with 20 Gy and administration of anti-CD73 (Fig. 5D). Forty-eight hours after injection, both tumors were harvested and analyzed for infiltration by the adoptively transferred cDC1s (CFSE^{+}CD103^{+}). CD73 blockade significantly enhanced cDC1 infiltration in irradiated but not untreated tumors (Fig. 5E–F). These results indicate that cDC1 homing to TSA tumors requires chemotactic and/or survival signals induced by radiotherapy together with blockade of adenosine generation.

CD73 blockade enhances abscopal responses in mice treated with 20 Gy radiotherapy and CTLA-4-blockade

4T1 is a poorly immunogenic model of TNBC resistant to ICB that seeds spontaneous metastases to the lungs; metasteses are present by the time the primary tumor is palpable (39). We have previously shown that radiotherapy used at 8 to 12 Gy dose per fraction, delivered in consecutive days 2–3 times, is synergistic with CTLA-4 and induces CD8^{+} T cell responses that control non-irradiated lung metastases (40). Similarly to TSA cells, 4T1 cells do not show radiotherapy-induced IFN-I production or priming of antitumor CD8^{+} T cells when treated with single-dose 20 Gy radiotherapy (9). Since CD73 was upregulated on 4T1 cells by radiotherapy (Fig. 2C and D), we asked if CD73 blockade could improve the local and systemic response of mice bearing 4T1 tumors treated with 20 Gy radiotherapy. Blockade of CD73, beginning when tumors were palpable, had no effect on the primary tumor or lung metastases (Fig. 6, A-B). When used with 20 Gy radiotherapy, CD73 blockade enhanced control of the irradiated tumor but not of lung metastases, suggesting that the immune response elicited by 20 Gy + CD73 blockade was not systemically effective. Therefore, we tested whether addition of CTLA-4 blockade could improve the control of the non-irradiated metastases in the lungs of mice treated with 20 Gy + CD73 blockade. The double blockade of CD73 and CTLA-4 had no effect without radiotherapy, but resulted in a significant decrease in lung metastases when combined with 20 Gy radiotherapy (Fig. 6B).

These results confirm the benefits of blocking adenosine generation to improve responses to radiotherapy. In addition, they show that CD73 blockade induces systemic antitumor immune responses in mice treated with a radiotherapy dose that is otherwise unable to induce abscopal effects in combination with anti-CTLA-4 (9).

CD73 blockade promotes cDC1 recruitment to irradiated tumors and improves abscopal response

CGAS-deficient TSA tumors cannot produce IFN-I in response to 8 Gy×3 radiotherapy and fail to induce tumor-specific CD8^{+} T cell activation and abscopal responses in combination with CTLA-4-blockade (9). Given the ability of CD73 blockade to induce the recruitment of cDC1 to tumors treated with 20 Gy, a radiotherapy dose that does not induce IFN-I (9), we hypothesized that CD73 blockade could complement the lack of IFN-I induction by 8 Gy×3 radiotherapy when the irradiated tumor was cGAS-deficient. In order to test this hypothesis,

we employed an abscopal tumor model in which TSA cells, transduced with doxycycline-inducible shRNA expression vectors directed against cGAS (TSA^{shcGAS}) or a non-silencing sequence (TSA^{shNS}), are injected in the right flank of WT BALB/c mice (primary tumor) followed by injection of TSA^{shNS} in the contralateral flank (abscopal tumor) (9). Primary tumors were irradiated with 8 Gy×3, and mice received anti-CD73 and/or anti-CTLA-4 (Fig. 7A). As expected, radiotherapy was effective at controlling the irradiated tumors regardless of cGAS expression (Supplementary Fig. S7), but did not induce abscopal responses. Consistently with prior results, CTLA-4-blockade with radiotherapy induced abscopal responses and increased significantly the survival of mice bearing TSA^{shNS} but not TSA^{shcGAS} primary tumors (9). CD73 blockade with radiotherapy did not induce abscopal responses in mice bearing TSA^{shNS} or TSA^{shcGAS} primary tumors (Fig. 7B). However, CD73 blockade restored the ability of the combination of 8 Gy×3 radiotherapy and CTLA-4-blockade to induce abscopal responses and extend survival of mice with TSA^{shcGAS} primary tumors (Fig. 7B–C). These data indicate that CD73 blockade is insufficient to induce abscopal responses in combination with radiotherapy, but can complement the defective activation of IFN-I by radiotherapy in tumors with downregulated cGAS expression.

Next, we sought to test whether CD73 blockade could promote the recruitment of cDC1 to cGAS-deficient tumors. We analyzed primary TSA^{shNS} and TSA^{shcGAS} tumors from mice treated with or without CD73 blockade for the presence of cDC1 five days following completion of 8 Gy×3 radiotherapy. As expected, 8 Gy×3 radiotherapy increased cDC1 in TSA^{shNS} tumors but not in TSA^{shcGAS} tumors (Fig. 7D) (9). CD73 blockade did not further increase cDC1 in irradiated TSA^{shNS} tumors but restored radiotherapy-induced cDC1 increases in TSA^{shcGAS} tumors (Fig. 7D). cDC1 recruitment to tumors treated with 8 Gy×3 is mediated by IFN-I and requires host expression of the IFN-I receptor (9). To determine whether cDC1 recruitment mediated by radiotherapy in the presence of CD73 blockade was independent from IFN-I, we performed an adoptive transfer experiment. cDC1s were obtained by culture of bone marrow cells derived from $Ifnar1^{-/-}$ mice or from WT mice. After CFSE labeling, cDC1 were injected i.v. into WT mice bearing TSA tumors treated with 20 Gy or 8 Gy×3 radiotherapy, then, 48 hours later, measured the number of $CFSE^{+}$ cDC1 cells infiltrating the irradiated tumors by flow cytometry. In line with previous findings (9), WT cDC1 homed in significantly higher numbers to tumors treated with 8 Gy×3 than 20 Gy radiotherapy (Fig. 7E). In contrast, homing of $Ifnar^{-/-}$ cDC1 to tumors treated with 8 Gy×3 radiotherapy was not increased. CD73 blockade did not further increase homing of WT cDC1 to tumors treated with 8 Gy×3, but restored homing of WT cDC1 to tumors treated with 20 Gy and restored homing of the $Ifnar^{-/-}$ cDC1 to tumors treated with either 8 Gy×3 radiotherapy or 20 Gy radiotherapy (Fig. 7E). Thus, when IFN-I-driven recruitment of cDC1 to tumors is hampered, an alternative pathway for cDC1 recruitment can be activated by radiotherapy and regulated by adenosine.

Our results show that CD73 regulates *in situ* vaccination by radiotherapy and radiotherapy enhances responses of breast cancer to ICB.

Discussion

Recruitment of cDC1 to the tumor is essential for development of spontaneous antitumor $CD8^+$ T cells, and cDC1 exclusion is one of the mechanisms responsible for the “cold” immunological phenotype characteristic of tumors resistant to ICB therapy (41–43). Focal radiotherapy enhances responses of poorly immunogenic “cold” tumors to ICB therapy at least in part by promoting recruitment and maturation of cDC1 (9). Radiotherapy-induced IFN-I plays a role in priming of antitumor T cells by radiotherapy; data suggest that this mechanism is clinically relevant (6,8,9,44). IFN-I provides a signal for cDC1 recruitment to the tumor (41). We and others have demonstrated that IFN-I production by cancer cells is mediated by radiotherapy-induced activation of the cGAS/STING pathway by self DNA that accumulates in the cytosol (9,10). Here we describe an alternative pathway for the recruitment of cDC1 to irradiated tumors that is independent of IFN-I and is regulated by CD73.

Blockade of CD73 had no effect on tumor growth by itself or in combination with anti-CTLA-4 in two tumor models of metastatic breast cancer. However, when combined with a radiotherapy dose of 20 Gy, which is unable to induce IFN-I production by the irradiated cancer cells (9), CD73 blockade improved control of the irradiated tumor and, in combination with CTLA-4-blockade, non-irradiated lung metastases (9). Likewise, when cGAS-deficient TSA tumors were treated with 8 Gy×3 radiotherapy and CTLA-4-blockade, CD73 blockade restored the induction of abscopal responses and improved mice survival. These results have clinical implications as many tumors epigenetically downregulate expression of cGAS and/or STING and may not be able to produce IFN-I in response to radiotherapy (12). In a clinical trial testing the combination of radiotherapy and the anti-CTLA-4 antibody ipilimumab in metastatic lung patients, we found that increased serum IFN-I after radiotherapy predicted an abscopal responses (6). Reasons for the failure of radiotherapy to induce IFN-I in non-responding patients are unclear, but it is possible that downregulation of cGAS/STING hindered the response, and that these patients could have benefited from treatment with CD73 blocking antibodies.

Radiotherapy-induced factors that promote tumor infiltration by cDC1 in the absence of IFN-I remain to be defined. Extracellular nucleotides mediate chemotaxis of DCs (45), and ATP released following chemotherapy mediated DC-recruitment to the tumor in vivo (15,46). In vitro, radiotherapy induced dose-dependent release of ATP by tumor cells (47), suggesting that ATP could mediate cDC1 recruitment to irradiated tumors. Conversion of ATP to adenosine may also affect the balance of activating and suppressive signals that regulate the retention, activation and survival of cDC1 within the irradiated tumor microenvironment (48). Further studies are required to define the effect of CD73 blockade on these processes in the irradiated tumor microenvironment.

Expression of CD73 on cancer cells inhibits tumor rejection by adoptively transferred antitumor T cells (49). We found that CD73 expressed on mouse and human breast cancer cells is upregulated by radiation. Knockdown of CD73 did not affect TSA tumor in the absence of radiotherapy, but enhanced tumor control in concert with radiotherapy. Thus, radiation-induced T cell activation as dependent on cDC1 is necessary, an interpretation

supported by loss of the therapeutic synergy between CD73 blockade and radiotherapy in Batf3$^{-/-}$ mice.

Radiotherapy increased expression of CD38 by mouse and human breast cancer cells, suggesting that the non-canonical pathway may contribute to the generation of adenosine induced by radiotherapy. CD38 has been implicated in generation of adenosine in melanoma, and upregulation of CD38 on tumor cells plays a role in resistance to anti–PD-1/PD-L1 therapy (17,25). Together with a known role of radiotherapy in disrupting NAD$^+$ metabolism, these data support the hypothesis that NAD$^+$ may be a source of adenosine in the irradiated tumor (50).

Expression of CD73 in TNBC is associated with a poor prognosis and poor response to neoadjuvant chemotherapy (22). Our preclinical data indicate that CD73 expression also reduces breast cancer response to radiotherapy, thus precluding the synergy of radiotherapy with ICB therapy in tumors unable to activate IFN-I. The observed increase in plasma sCD73 after radiotherapy in metastatic breast cancer patients supports the concept that this pathway should be targeted in the clinic to improve responses, especially when radiotherapy is used in combination with ICB. sCD73 expression in breast cancer patients and its modulation by radiotherapy should be explored as a potential biomarker predictive of response.

In summary, we have identified a role for the adenosinergic pathway in regulating radiotherapy-induced *in situ* vaccination by limiting cDC1 infiltration in conditions of suboptimal IFN-I induction by radiotherapy. Clinical trials are underway to assess safety and efficacy of CD73 blocking antibodies alone or in combination with ICB in patients with advanced solid tumors (26). Our findings provide the rationale for testing CD73 blockade in patients who carry cGAS/STING$^-$ tumors or show upregulation of sCD73 following radiotherapy to determine if CD73 blockade can enhance responses to ICB.

Supplementary Material

Refer to Web version on PubMed Central for supplementary material.

Acknowledgments:

We thank Dr. Fabio Malavasi for helpful discussions ,Bruce Cronstein for adenosine measurement help, Barbara Maier and Miriam Merad for cDC1 generation and identification protocols, and Andreas Lundqvist for critically reviewing the manuscript.

Grant support: This study was supported by Department of Defense, Breast Cancer Research Program Breakthrough Fellowship Award W81XWH-17-1-0029 to EW and Multi-Team Award W81XWH-11-1-0530 to SCF, and by NIH R01 CA201246 to SD. Additional funding was provided by grants from the Breast Cancer Research Foundation (BCRF-16-054 and BCRF-17-053) to SD and SCF.

References

1. Ribas A, Wolchok JD. Cancer immunotherapy using checkpoint blockade. Science 2018;359(6382):1350–5 doi 10.1126/science.aar4060. [PubMed: 29567705]
2. Sharma P, Allison JP. The future of immune checkpoint therapy. Science 2015;348(6230):56–61 doi 10.1126/science.aaa8172. [PubMed: 25838373]

3. Demaria S, Golden EB, Formenti SC. Role of Local Radiation Therapy in Cancer Immunotherapy. JAMA Oncol 2015;1(9):1325–32 doi 10.1001/jamaoncol.2015.2756. [PubMed: 26270858]
4. Kang J, Demaria S, Formenti S. Current clinical trials testing the combination of immunotherapy with radiotherapy. J Immunother Cancer 2016;4:51 doi 10.1186/s40425-016-0156-7.. [PubMed: 27660705]
5. Twyman-Saint Victor C, Rech AJ, Maity A, Rengan R, Pauken KE, Stelekati E, et al. Radiation and dual checkpoint blockade activate non-redundant immune mechanisms in cancer. Nature 2015;520(7547):373–7. [PubMed: 25754329]
6. Formenti SC, Rudqvist NP, Golden E, Cooper B, Wennerberg E, Lhuillier C, et al. Radiotherapy induces responses of lung cancer to CTLA-4 blockade. Nat Med 2018;24(12):1845–51 doi 10.1038/s41591-018-0232-2. [PubMed: 30397353]
7. Wennerberg E, Lhuillier C, Vanpouille-Box C, Pilones KA, Garcia-Martinez E, Rudqvist NP, et al. Barriers to Radiation-Induced In Situ Tumor Vaccination. Front Immunol 2017;8:229 doi 10.3389/fimmu.2017.00229. [PubMed: 28348554]
8. Burnette BC, Liang H, Lee Y, Chlewicki L, Khodarev NN, Weichselbaum RR, et al. The efficacy of radiotherapy relies upon induction of type i interferon-dependent innate and adaptive immunity. Cancer Res 2011;71(7):2488–96 doi 10.1158/0008-5472.CAN-10-2820. [PubMed: 21300764]
9. Vanpouille-Box C, Alard A, Aryankalayil MJ, Sarfraz Y, Diamond JM, Schneider RJ, et al. DNA exonuclease Trex1 regulates radiotherapy-induced tumour immunogenicity. Nat Commun 2017;8:15618 doi 10.1038/ncomms15618. [PubMed: 28598415]
10. Harding SM, Benci JL, Irianto J, Discher DE, Minn AJ, Greenberg RA. Mitotic progression following DNA damage enables pattern recognition within micronuclei. Nature 2017;548(7668):466–70 doi 10.1038/nature23470. [PubMed: 28759889]
11. Hildner K, Edelson BT, Purtha WE, Diamond M, Matsushita H, Kohyama M, et al. Batf3 deficiency reveals a critical role for CD8alpha+ dendritic cells in cytotoxic T cell immunity. Science 2008;322(5904):1097–100 doi 10.1126/science.1164206. [PubMed: 19008445]
12. Konno H, Yamauchi S, Berglund A, Putney RM, Mule JJ, Barber GN. Suppression of STING signaling through epigenetic silencing and missense mutation impedes DNA damage mediated cytokine production. Oncogene 2018;37(15):2037–51 doi 10.1038/s41388-017-0120-0. [PubMed: 29367762]
13. Golden EB, Apetoh L. Radiotherapy and immunogenic cell death. Semin Radiat Oncol 2015;25(1):11–7 doi 10.1016/j.semradonc.2014.07.005. [PubMed: 25481261]
14. Aymeric L, Apetoh L, Ghiringhelli F, Tesniere A, Martins I, Kroemer G, et al. Tumor cell death and ATP release prime dendritic cells and efficient anticancer immunity. Cancer Res 2010;70(3):855–8 doi 10.1158/0008-5472.CAN-09-3566. [PubMed: 20086177]
15. Saez PJ, Vargas P, Shoji KF, Harcha PA, Lennon-Dumenil AM, Saez JC. ATP promotes the fast migration of dendritic cells through the activity of pannexin 1 channels and P2X7 receptors. Sci Signal 2017;10(506) doi 10.1126/scisignal.aah7107.
16. Young A, Mittal D, Stagg J, Smyth MJ. Targeting cancer-derived adenosine: new therapeutic approaches. Cancer Discov 2014;4(8):879–88 doi 10.1158/2159-8290.CD-14-0341. [PubMed: 25035124]
17. Morandi F, Morandi B, Horenstein AL, Chillemi A, Quarona V, Zaccarello G, et al. A non-canonical adenosinergic pathway led by CD38 in human melanoma cells induces suppression of T cell proliferation. Oncotarget 2015;6(28):25602–18 doi 10.18632/oncotarget.4693. [PubMed: 26329660]
18. Horenstein AL, Chillemi A, Zaccarello G, Bruzzone S, Quarona V, Zito A, et al. A CD38/CD203a/CD73 ectoenzymatic pathway independent of CD39 drives a novel adenosinergic loop in human T lymphocytes. Oncoimmunology 2013;2(9):e26246 doi 10.4161/onci.26246. [PubMed: 24319640]
19. Ohta A, Gorelik E, Prasad SJ, Ronchese F, Lukashev D, Wong MK, et al. A2A adenosine receptor protects tumors from antitumor T cells. Proc Natl Acad Sci U S A 2006;103(35):13132–7 doi 10.1073/pnas.0605251103. [PubMed: 16916931]
20. Novitskiy SV, Ryzhov S, Zaynagetdinov R, Goldstein AE, Huang Y, Tikhomirov OY, et al. Adenosine receptors in regulation of dendritic cell differentiation and function. Blood 2008;112(5):1822–31 doi 10.1182/blood-2008-02-136325. [PubMed: 18559975]

21. Zarek PE, Huang CT, Lutz ER, Kowalski J, Horton MR, Linden J, et al. A2A receptor signaling promotes peripheral tolerance by inducing T-cell anergy and the generation of adaptive regulatory T cells. Blood 2008;111(1):251–9 doi 10.1182/blood-2007-03-081646. [PubMed: 17909080]
22. Loi S, Pommey S, Haibe-Kains B, Beavis PA, Darcy PK, Smyth MJ, et al. CD73 promotes anthracycline resistance and poor prognosis in triple negative breast cancer. Proc Natl Acad Sci U S A 2013;110(27):11091–6 doi 10.1073/pnas.1222251110. [PubMed: 23776241]
23. Jiang T, Xu X, Qiao M, Li X, Zhao C, Zhou F, et al. Comprehensive evaluation of NT5E/CD73 expression and its prognostic significance in distinct types of cancers. BMC Cancer 2018;18(1):267 doi 10.1186/s12885-018-4073-7. [PubMed: 29514610]
24. Buisseret L, Pommey S, Allard B, Garaud S, Bergeron M, Cousineau I, et al. Clinical significance of CD73 in triple-negative breast cancer: multiplex analysis of a phase III clinical trial. Ann Oncol 2018;29(4):1056–62 doi 10.1093/annonc/mdx730. [PubMed: 29145561]
25. Chen L, Diao L, Yang Y, Yi X, Rodriguez BL, Li Y, et al. CD38-Mediated Immunosuppression as a Mechanism of Tumor Cell Escape from PD-1/PD-L1 Blockade. Cancer Discov 2018;8(9):1156–75 doi 10.1158/2159-8290.CD-17-1033. [PubMed: 30012853]
26. Allard D, Chrobak P, Allard B, Messaoudi N, Stagg J. Targeting the CD73-adenosine axis in immuno-oncology. Immunol Lett 2019;205:31–9 doi 10.1016/j.imlet.2018.05.001. [PubMed: 29758241]
27. Aslakson CJ, Miller FR. Selective events in the metastatic process defined by analysis of the sequential dissemination of subpopulations of a mouse mammary tumor. Cancer Res 1992;52:1399–405. [PubMed: 1540948]
28. Rosato A, Santa SD, Zoso A, Giacomelli S, Milan G, Macino B, et al. The cytotoxic T-lymphocyte response against a poorly immunogenic mammary adenocarcinoma is focused on a single immunodominant class I epitope derived from the gp70 Env product of an endogenous retrovirus. Cancer Res 2003;63:2158–63. [PubMed: 12727834]
29. Lutz MB, Kukutsch N, Ogilvie AL, Rossner S, Koch F, Romani N, et al. An advanced culture method for generating large quantities of highly pure dendritic cells from mouse bone marrow. J Immunol Methods 1999;223(1):77–92. [PubMed: 10037236]
30. Mayer CT, Ghorbani P, Nandan A, Dudek M, Arnold-Schrauf C, Hesse C, et al. Selective and efficient generation of functional Batf3-dependent CD103+ dendritic cells from mouse bone marrow. Blood 2014;124(20):3081–91 doi 10.1182/blood-2013-12-545772. [PubMed: 25100743]
31. Chen Q, Deeb RS, Ma Y, Staudt MR, Crystal RG, Gross SS. Serum Metabolite Biomarkers Discriminate Healthy Smokers from COPD Smokers. PLoS One 2015;10(12):e0143937 doi 10.1371/journal.pone.0143937. [PubMed: 26674646]
32. Formenti SC, Lee P, Adams S, Goldberg JD, Li X, Xie MW, et al. Focal Irradiation and Systemic TGFbeta Blockade in Metastatic Breast Cancer. Clin Cancer Res 2018;24(11):2493–504 doi 10.1158/1078-0432.CCR-17-3322. [PubMed: 29476019]
33. Hasko G, Cronstein BN. Adenosine: an endogenous regulator of innate immunity. Trends Immunol 2004;25(1):33–9. [PubMed: 14698282]
34. Morello S, Capone M, Sorrentino C, Giannarelli D, Madonna G, Mallardo D, et al. Soluble CD73 as biomarker in patients with metastatic melanoma patients treated with nivolumab. J Transl Med 2017;15(1):244 doi 10.1186/s12967-017-1348-8. [PubMed: 29202855]
35. Airas L, Niemela J, Salmi M, Puurunen T, Smith DJ, Jalkanen S. Differential regulation and function of CD73, a glycosyl-phosphatidylinositol-linked 70-kD adhesion molecule, on lymphocytes and endothelial cells. J Cell Biol 1997;136(2):421–31. [PubMed: 9015312]
36. Regateiro FS, Cobbold SP, Waldmann H. CD73 and adenosine generation in the creation of regulatory microenvironments. Clin Exp Immunol 2013;171(1):1–7 doi 10.1111/j.1365-2249.2012.04623.x. [PubMed: 23199317]
37. Schaue D, Ratikan JA, Iwamoto KS, McBride WH. Maximizing tumor immunity with fractionated radiation. Int J Radiat Oncol Biol Phys 2012;83(4):1306–10 doi 10.1016/j.ijrobp.2011.09.049. [PubMed: 22208977]
38. Quezada SA, Peggs KS, Curran MA, Allison JP. CTLA4 blockade and GM-CSF combination immunotherapy alters the intratumor balance of effector and regulatory T cells. J Clin Invest 2006;116(7):1935–45. [PubMed: 16778987]

39. Pulaski BA, Ostrand-Rosenberg S. Mouse 4T1 breast tumor model. Curr Protoc Immunol 2001;Chapter 20:Unit 20 2 doi 10.1002/0471142735.im2002s39.
40. Demaria S, Kawashima N, Yang AM, Devitt ML, Babb JS, Allison JP, et al. Immune-mediated inhibition of metastases after treatment with local radiation and CTLA-4 blockade in a mouse model of breast cancer. Clin Cancer Res 2005;11(2 Pt 1):728–34. [PubMed: 15701862]
41. Diamond MS, Kinder M, Matsushita H, Mashayekhi M, Dunn GP, Archambault JM, et al. Type I interferon is selectively required by dendritic cells for immune rejection of tumors. J Exp Med 2011;208(10):1989–2003 doi 10.1084/jem.20101158. [PubMed: 21930769]
42. Spranger S, Bao R, Gajewski TF. Melanoma-intrinsic beta-catenin signalling prevents anti-tumour immunity. Nature 2015;523(7559):231–5 doi 10.1038/nature14404. [PubMed: 25970248]
43. Sharma P, Allison JP. Immune checkpoint targeting in cancer therapy: toward combination strategies with curative potential. Cell 2015;161(2):205–14 doi 10.1016/j.cell.2015.03.030. [PubMed: 25860605]
44. Deng L, Liang H, Xu M, Yang X, Burnette B, Arina A, et al. STING-Dependent Cytosolic DNA Sensing Promotes Radiation-Induced Type I Interferon-Dependent Antitumor Immunity in Immunogenic Tumors. Immunity 2014;41(5):843–52 doi 10.1016/j.immuni.2014.10.019. [PubMed: 25517616]
45. Idzko M, Dichmann S, Ferrari D, Di Virgilio F, la Sala A, Girolomoni G, et al. Nucleotides induce chemotaxis and actin polymerization in immature but not mature human dendritic cells via activation of pertussis toxin-sensitive P2y receptors. Blood 2002;100(3):925–32. [PubMed: 12130504]
46. Ma Y, Adjemian S, Yang H, Catani JP, Hannani D, Martins I, et al. ATP-dependent recruitment, survival and differentiation of dendritic cell precursors in the tumor bed after anticancer chemotherapy. Oncoimmunology 2013;2(6):e24568 doi 10.4161/onci.24568. [PubMed: 23894718]
47. Golden EB, Frances D, Pellicciotta I, Demaria S, Helen Barcellos-Hoff M, Formenti SC. Radiation fosters dose-dependent and chemotherapy-induced immunogenic cell death. Oncoimmunology 2014;3:e28518 doi 10.4161/onci.28518. [PubMed: 25071979]
48. de Leve S, Wirsdorfer F, Jendrossek V. Targeting the Immunomodulatory CD73/Adenosine System to Improve the Therapeutic Gain of Radiotherapy. Front Immunol 2019;10:698 doi 10.3389/fimmu.2019.00698. [PubMed: 31024543]
49. Jin D, Fan J, Wang L, Thompson LF, Liu A, Daniel BJ, et al. CD73 on tumor cells impairs antitumor T-cell responses: a novel mechanism of tumor-induced immune suppression. Cancer Res 2010;70(6):2245–55 doi 10.1158/0008-5472.CAN-09-3109. [PubMed: 20179192]
50. Lewis JE, Singh N, Holmila RJ, Sumer BD, Williams NS, Furdui CM, et al. Targeting NAD(+) Metabolism to Enhance Radiation Therapy Responses. Semin Radiat Oncol 2019;29(1):6–15 doi 10.1016/j.semradonc.2018.10.009. [PubMed: 30573185]

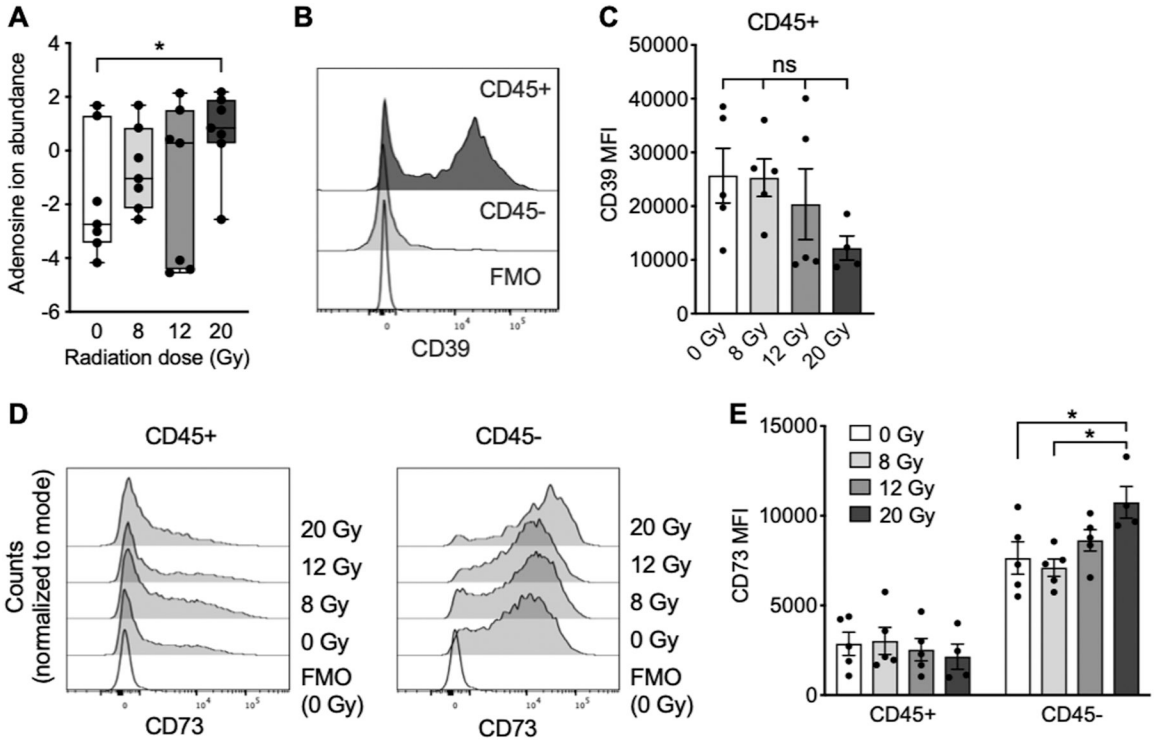

Figure 1. High dose radiotherapy (RT) induces adenosine increase in mouse tumors.

Mice bearing s.c. TSA tumors were treated with focal radiotherapy at different doses as indicated. Twenty-four hours after radiotherapy, tumors were harvested for analysis. (**A**) Adenosine ion abundance. Data was normalized to median and log2 transformed. Plot shows median values and interquartile range. $n = 7$ per group, Welch's t test, * $P<0.05$,. The experiment was performed twice with similar results. (**B, C**) Surface expression of CD39 on $CD45^+$ and $CD45^-$ cells. (**B**) Representative histograms and (**C**) mean fluorescence intensity (MFI) on $CD45^+$ cells. (**D, E**) Surface expression of CD73 on $CD45^+$ and $CD45^-$ cells. (**D**) Representative histograms and (**E**) MFI. Flow cytometry data shows mean±s.e.m. $n = 4–5$ per group, ANOVA followed by Tukey's test. ns = non-significant., * $P<0.05$.

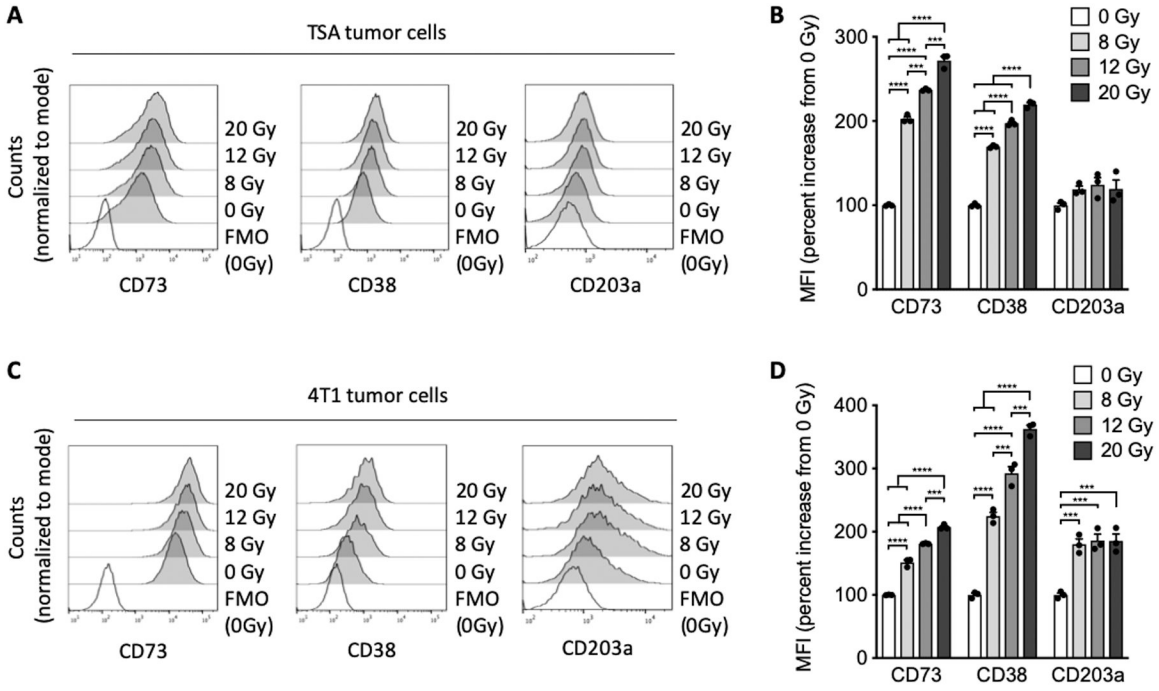

Figure 2. Radiation increases expression of non-canonical adenosine generation pathway by mouse breast cancer cells.

TSA and 4T1 tumor cells were treated with single doses of radiation, as indicated and analyzed 24 hours later by flow cytometry. (**A, B**) Expression of CD73, CD38 and CD203a on TSA tumor cells (n = 3 per group). (**A**) Representative histograms and (**B**) percent increase in MFI compared to mock-treated cells (0 Gy). (**C, D**) Expression of CD73, CD38 and CD203a on 4T1 tumor cells (n = 3 per group). (**C**) Representative histograms and (**D**) percent increase in MFI compared to mock-treated cells (0 Gy) .. All data shows mean ±s.e.m. ANOVA followed by Tukey's test. . * P<0.05, *** P<0.001, **** P<0.0001.

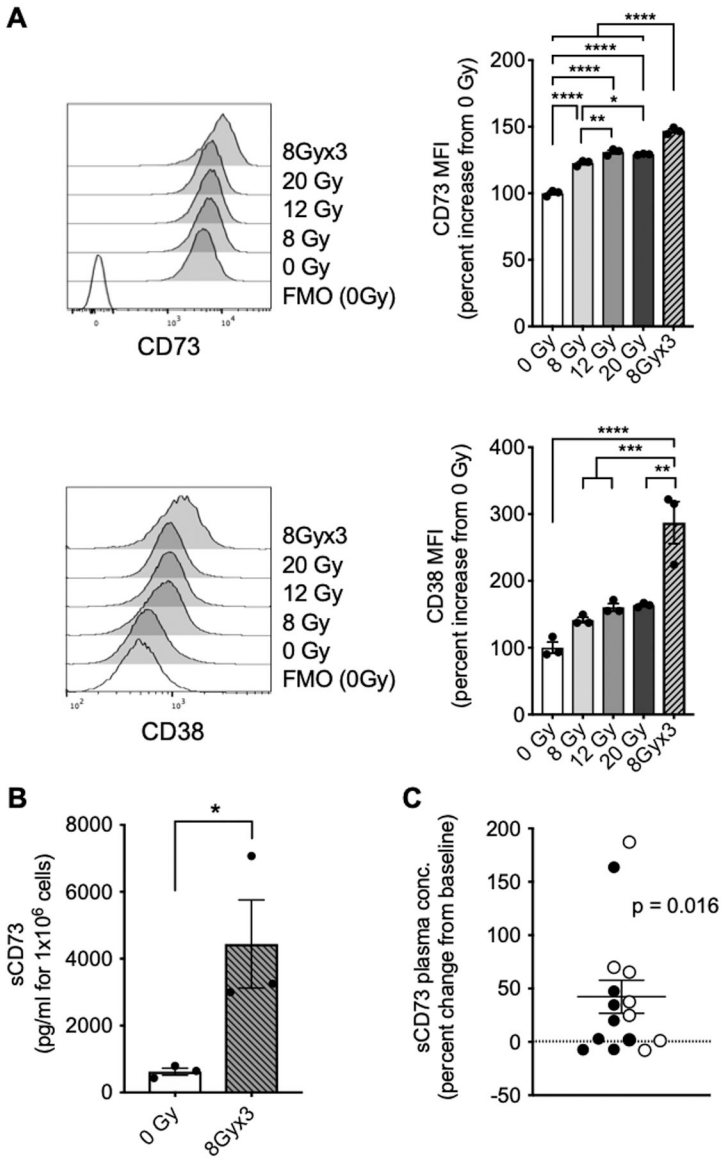

Figure 3. Radiation-induced upregulation of adenosine-generating ectonucleotidases in human breast cancer.

(**A**) Representative histograms depicting expression of CD73 (upper panel) and CD38 (lower panel) on MDA-MB-231 cells 24 hours post-treatment with radiation as indicated. Bar graphs show percent increase in MFI compared to mock-treated cells (0 Gy). (n = 3)ANOVA followed by Tukey's test. (**B**) Soluble CD73 (sCD73) in supernatants from MDA-MB-231 cells treated with radiation as indicated measured 24 hours after last radiation dose. (n = 3), unpaired t test. (**C**) Percent change in concentration of sCD73 in plasma samples from breast cancer patients (n = 15) two weeks following treatment with radiotherapy (7.5Gy×3) and fresolimumab (1 mg/kg [filled circles] or 10 mg/kg [open circles]) compared to baseline sCD73 concentration. Each symbol represents a patient (n = 15). One-sample t test. All data shows mean±s.e.m.* P<0.05, **** P<0.0001.

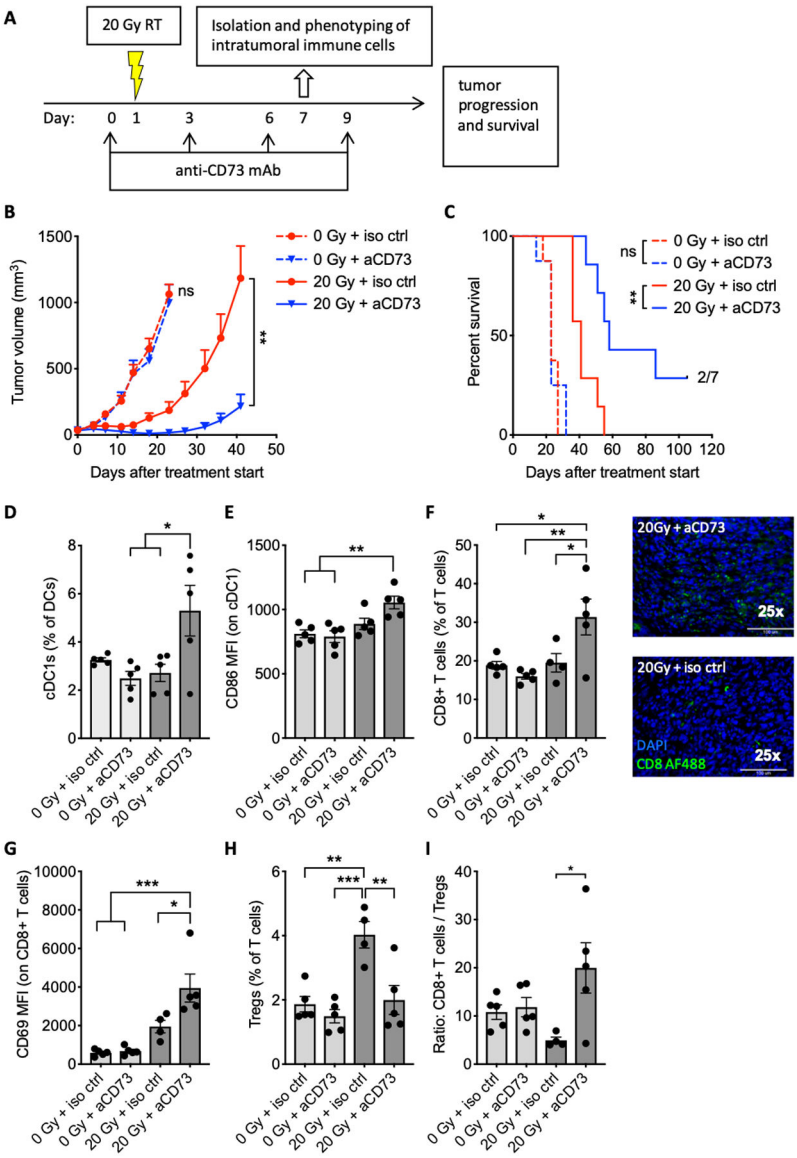

Figure 4. Blocking CD73 improved the response to 20 Gy radiotherapy, increased tumor infiltration by dendritic cells, and enhanced CD8$^+$/Treg cell ratio.

(**A**) Tumor treatment schema. Mice bearing TSA tumors were treated with 20 Gy radiotherapy and/or anti-CD73 or isotype control antibody, as indicated. Some mice were sacrificed on day 7 for flow cytometric analysis of intratumoral immune cells (n = 4–5 per group). The remaining mice (n = 7 per group) were followed for (**B**) tumor growth and (**C**) survival. Effect of anti-CD73 on tumor progression as assessed by repeated measure ANOVA in mock-treated mice (0 Gy) between day 0 (treatment start) and day 23 and in radiotherapy-treated mice (20 Gy) between day 0 and day 41. Log-rank test was used to assess effect of anti-CD73 on mouse survival for mice treated with the same radiotherapy treatment. The experiment was performed twice with similar results. (**D**) Frequency of cDC1 (CD8α^+) among DCs. (**E**) MFI of CD86 by DCs. (**F**) Percentage of CD8$^+$ T cells among T cells (left panel) and tumor infiltration of CD8$^+$ T cells in tumor sections stained as indicated (25X magnification) (right panel).. (**G**) MFI of CD69 on CD8$^+$ T cells. (**H**) Percentage of

Tregs among T cells. (**I**) Ratio of $CD8^+$ T cells to Tregs. Experiment was repeated 2–3 times with similar results.. ANOVA followed by Tukey's test. All data shows mean ± s.e.m. . * $P<0.05$, ** $P<0.01$, **** $P<0.0001$,

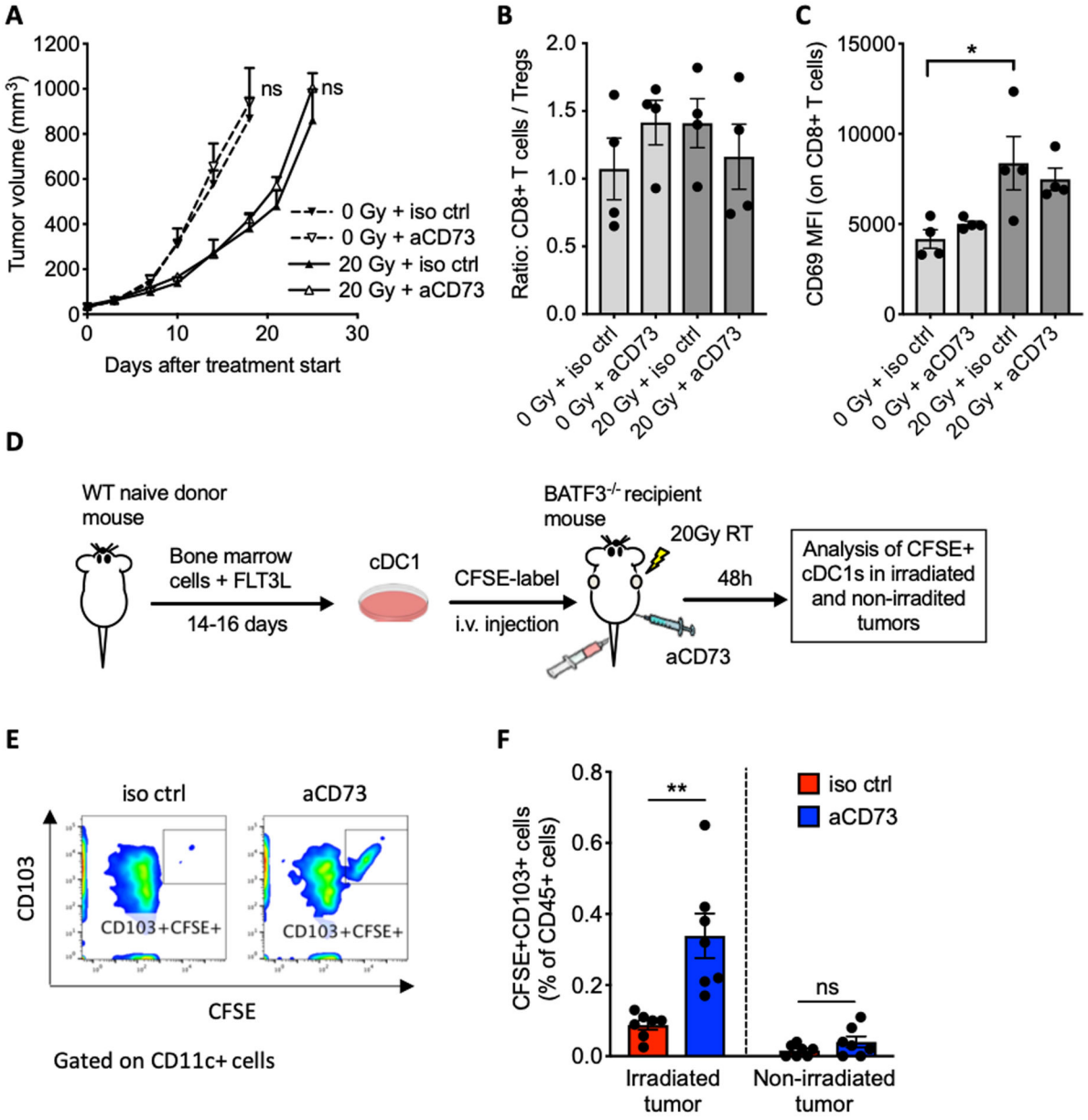

Figure 5. Synergy of 20 Gy radiotherapy with CD73 blockade depends on cDC1.

Batf3$^{-/-}$ mice were inoculated subcutaneously with TSA cells and treated with 20 Gy radiotherapy and anti-CD73 or isotype control as in Fig. 4A. (**A**) Mice were followed for tumor growth (n=5 per group). Effect of anti-CD73 on tumor progression was assessed by repeated measure ANOVA in mock-treated mice (0 Gy) between day 0 (treatment start) and day 18 and in radiotherapy-treated mice (20 Gy) between day 0 and day 25. (**B, C**) Some mice were sacrificed on day 7 for analysis of intratumoral immune cells (n=4). (**B**) Ratio of CD8$^+$ T cells to Treg cells and (**C**) MFI of CD69 on CD8$^+$ T cells.. ANOVA followed by Tukey's test. (**D**) Experimental schema for the cDC1 adoptive transfer. Bone-marrow cells were from wild type (WT) mice were cultured with FLT3L and GM-CSF to generate CD103$^+$ cDC1s. cDC1s were labeled with CFSE before i.v. injections into Batf3-deficient (Batf3$^{-/-}$) mice bearing two TSA tumors, 6 hours after irradiation of one tumor with 20 Gy

and anti-CD73 or control mAb administration. Irradiated and non-irradiated tumors were harvested 48 hours after adoptive transfer for flow cytometry analysis . (**E**) Representative dot plots of intratumoral $CD11c^+$ cells analyzed for expression of CFSE and CD103. (**F**) Frequency of $CFSE^+CD103^+$ cDC1s among total viable leukocytes in irradiated tumors and non-irradiated tumors (n=7 per group), Welch's t test., All data shows mean±s.e.m. *P<0.01, ** P<0.01

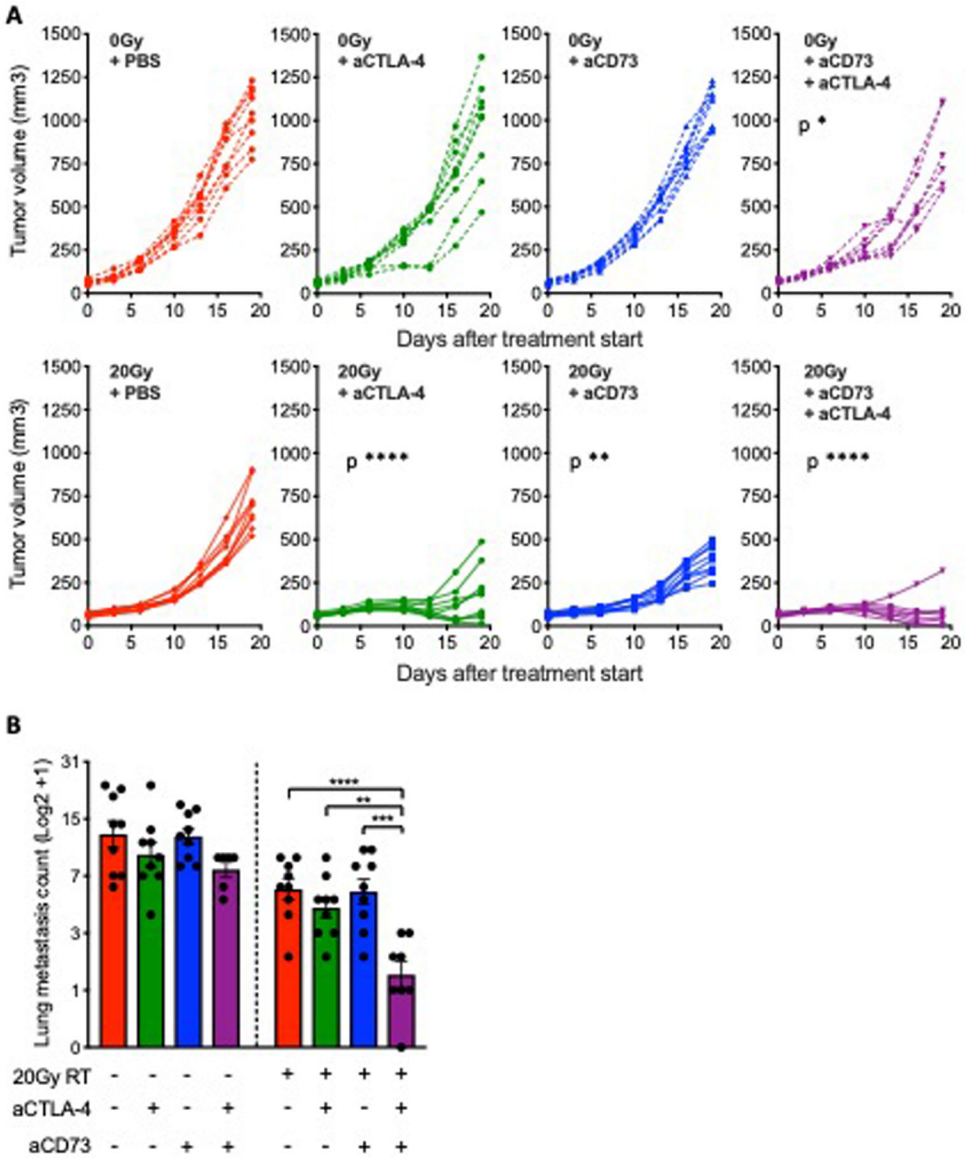

Figure 6. CD73 blockade in combination with anti-CTLA-4 enhanced 4T1 tumor response to radiotherapy and inhibited lung metastases.

BALB/c mice were inoculated subcutaneously with 4T1 cells in the right flank. Treatment with anti-CD73 was started when average tumor volumes approached 40–60 mm^3 (day 0) and repeated on day 3, 6 and 9. Radiotherapy was given as a single 20 Gy dose to the tumor on day 1. Anti-CTLA-4 was administered on day 1, 4 and 7. (**A**-**B**) Mice were followed for tumor growth and euthanized on day 19 for assessment of lung metastases . (**A**) Tumor progression in individual mice. Statistical significance was assessed by repeated measure ANOVA. Asterisks indicate P values for the comparison of each treatment group versus PBS-treated controls for mice treated with the same radiotherapy treatment. (**B**) Number of lung metastasis on day 19 after treatment start (n=6–9 per group). Metastases counts were log_2 transformed.ANOVA followed by Tukey's test. All data shows mean ± s.e.m.. * P<0.05, ** P<0.01, *** P<0.001, **** P<0.0001.

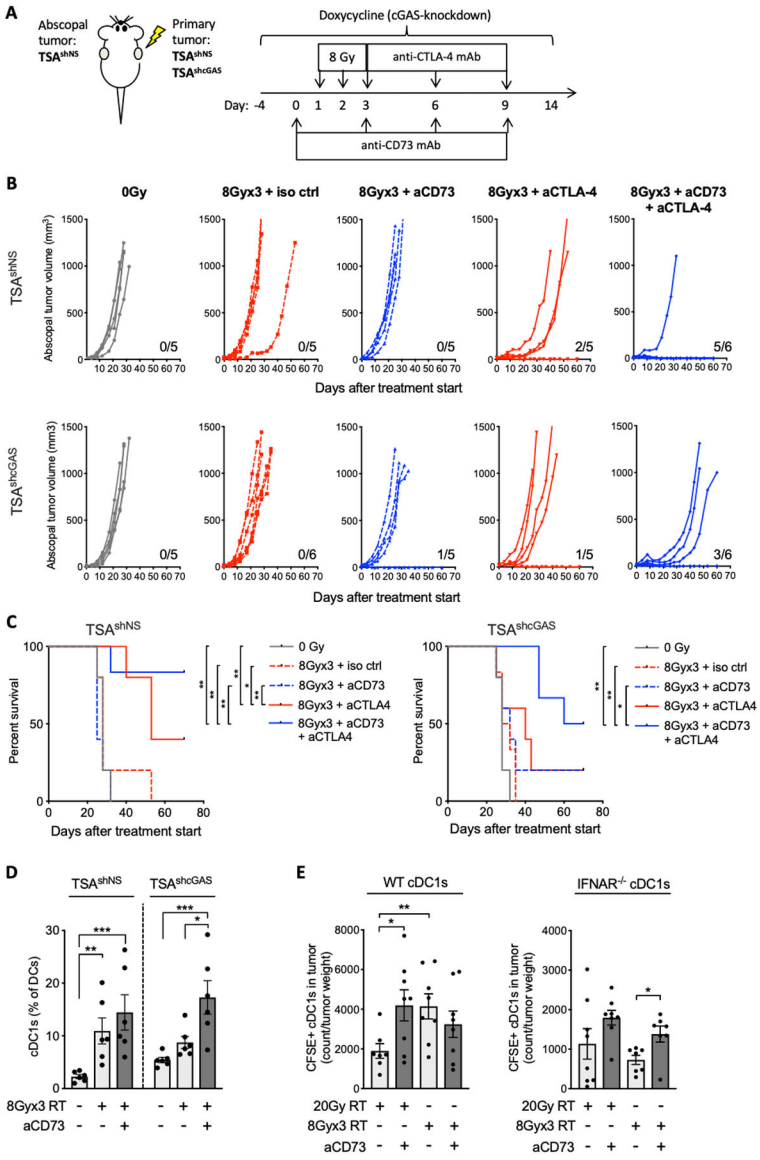

Figure 7. CD73 blockade improved induction of abscopal response upon irradiation of cGAS-deficient tumors and restored impaired recruitment of cDC1 to cGAS-deficient tumors following radiotherapy.

(**A**) Experimental schema. TSA cells expressing a doxycyclin-inducible short hairpin RNA (shRNA) directed against cGAS (TSA^{shcGAS}) or a non-silencing sequence (TSA^{shNS}) were injected in the right flank of WT BALB/c mice (primary tumors). Two days later TSA^{shNS} cells were injected in the contralateral flank (abscopal tumors). Doxycyclin was fed to mice once the tumors became palpable (day −4) and treatment started when primary tumors reached a volume of 40–60 mm^3 (day 0). Radiotherapy was given in 3 daily doses of 8 Gy to the primary tumor. Anti-CD73 and anti-CTLA-4 mAb were administered i.p. as indicated, and mice followed for tumor growth and survival. (**B**) Abscopal tumor growth over time. Each line represents an individual mouse (n=5–6). Numbers indicate the number of mice with complete tumor regression over the total in each group. (**C**) Survival in mice bearing primary TSA^{shNS} tumors or TSA^{shcGAS} tumors. Log-rank (Mantel-Cox) test . (**D**) WT

BALB/c mice were inoculated with primary TSA^{shNS} or TSA^{shcGAS} tumors and treated as above with radiotherapy and CD73 blockade. Tumors were harvested 5 days after last dose of radiotherapy for analysis of percentage of cDC1 ($XCR1^{+}CD8\alpha^{+}$) among total DCs (n=6 per group), ANOVA . Experiment was performed twice with similar results. (**E**) cDC1s prepared from the bone marrow of WT or $Ifnar^{-/-}$ mice were labeled with CSFE and adoptively transferred into WT BALB/c mice bearing TSA tumors 6 hours after irradiation with 20 GyX1 or 8 Gy×3 and/or anti-CD73 administration. Tumors harvested 48 hours later were evaluated for CFSE-labeled cDC1 infiltration. Bar graphs show the number of CFSE $^{+}CD11c^{+}$ cells normalized to tumor weight in mice receiving WT cDC1s (left panel) and $Ifnar^{-/-}$ cDC1s (right panel) (n=7–8). Welch's *t* test. Data were square root transformed prior to statistical testing. All data shows mean ± s.e.m.,* $P<0.05$, ** $P<0.01$, *** $P<0.001$.